

FR 7601696

RECOIL-DISTANCE LIFETIME MEASUREMENTS OF
STATES IN ^{47}V AND ^{47}Ti INDUCED BY HEAVY-
ION REACTIONS.

M. TOULEMONDE, N. SCHULZ, J. C. MERDINGER and
P. ENGELSTEIN

Laboratoire de Physique du Noyau et de Physique des
Particules/ PN

Institut National
de Physique Nucléaire
et de Physique
des Particules

Université
Louis Pasteur
de Strasbourg

RECOIL-DISTANCE LIFETIME MEASUREMENTS OF STATES IN
 ^{41}V AND ^{47}Ti INDUCED BY HEAVY-ION REACTION

M. TOULEMONDE, N. SCHULZ, J. C. MEBDINGER and PENDELSTEIN

Centre de Recherches Nucléaires et Université de Louis
Pasteur, Strasbourg, France

Abstract The recoil-distance method has been used in conjunction with heavy-ion reactions to measure the following mean lives:

$\tau = 1.24 \pm 0.16$ ns and 0.67 ± 0.11 ns for the 88-keV $3/2^+$ and 146-keV 2^+ states in ^{47}V , and $\tau = 314 \pm 22$ ps for the 160-keV 2^+ state in ^{47}Ti .

NUCLEAR REACTIONS $^{31}\text{P}(^{19}\text{F},\alpha)^{47}\text{V}$, $^{46}\text{Ti}(\alpha,p)^{47}\text{V}$; $E = 47$ MeV; measured recoil-distance; ^{47}V , ^{47}Ti levels deduced; $T_{1/2}^{\text{exp}}$ (B-M1, B-E2); Natural target; Ge(Li) detector.

1. INTRODUCTION

Evidence for deformation of the even-even nuclei in the middle of the $1f_{7/2}$ shell already exists. The energy of the first 2^+ states decreases from the nuclei with doubly closed shells towards the center of the shell and the strength of the corresponding $E2, 2^+ \rightarrow 0^+$ transition increases¹⁾. Less information is available for the odd-A nuclei. Among them, ^{47}V represents a very peculiar case because it is the only nucleus in this region known to have a ground state with spin and parity $3/2^-$. This feature is not reproduced by simple $(1f_{7/2})^1$ calculations, whatever two-body matrix elements are used²⁾. Recently spin assignments, branching ratios, multipole mixing ratios and lifetimes for low-lying levels of ^{47}V have become available mainly through the studies²⁻⁴⁾ of the $^{47}\text{Ti}(p,ny)$ and $^{40}\text{Ca}(^{16}\text{O},n2p\gamma)$ reactions. In the present work, the lifetimes of the two first excited states of ^{47}V are measured with the recoil-distance technique in the $^{31}\text{P}(^{19}\text{F},p2n)$ reaction. In addition, a precise value for the lifetime of the first excited state in ^{47}Ti , populated via the $^{31}\text{P}(^{19}\text{F},n2p)$ reaction, is obtained.

II. EXPERIMENTAL ARRANGEMENT AND DATA ANALYSIS.

Lifetimes were measured with a plunger apparatus similar to the one described elsewhere⁵⁾. The target consisted of a $250 \mu\text{g cm}^{-2}$ thick layer of Zn_3P_2 evaporated onto a 1 mg cm^{-2} thick Au foil. A thicker circular Au foil, of 5.2 cm diameter, was used to stop the recoiling nuclei. A 47-MeV ^{19}F -beam from the MP tandem Van de Graaff was used to populate the levels of interest. The γ -ray spectra were measured with a 3.1 cm^3 Ge(Li) detector at 0° with respect to the beam. Under actual running conditions, the resolution width of the Ge(Li) detector was 1 keV for a 88-keV γ -ray line.

Since in the present experiment the recoil distances D were not always negligible compared to the target-detector distance, the variation of the solid angle had to be taken into account. The photopiez efficiency of the counter versus distance r from the source was determined by using the 81-keV γ -ray of ^{132}Ba . Following the method outlined by Goosman and Kavanagh²⁾, the numbers of counts versus r were fitted by a function $Ae^{-\alpha r}$, A being a constant. A value of $\alpha = 0.225 \pm 0.011 \text{ cm}^{-1}$ was obtained from this fit.

The γ -ray data for the 160-keV transition in ^{47}Ti are shown in the left half of Fig. 1 for three target stopper distances $D = d - d_0$, d being the reading of the micrometer which positions the stopper and d_0 the reading for zero target-stopper distance. The peak areas I_0 and I_s for the unshifted and shifted lines were extracted from these spectra by subtracting an exponential background. The area of the shifted component has to be corrected for the energy dependance of the Ge(Li) detector efficiency and for the large solid angle due to the nuclei's motion. The two effects, which are of opposite sign, cancel to within 1% in the present experiment where a mean recoil velocity $v = 0.0268 c$ is determined from the difference in centroid energies of the two components. A small background in the unshifted component is observed at large D distances. If this background is due to cascade feeding from a long-lived level or from radioactivity on the stopper, the area I_0 may be expressed as :

$$I_0 = N \int_0^\infty e^{-(D/v\tau)(1-\alpha v\tau)} \cdot C e^{-\lambda x} dx \quad (1)$$

where τ is the mean-life of the level under study and N a normalisation constant for each value of D . In the present experiment, comparable yields for the $n2p$ and $p2n$ evaporation processes were observed. Since only 0.1% of the β -decay⁷⁾ of ^{47}V is feeding the 160-keV level in ^{47}Ti , this may not be the main process producing the background. If it is

supposed that background is due to the γ -radiation from a source whose lifetime is short compared to the transit time of the ions in the target material, the quantity $Ce^{D\alpha}$ in Eq. (1) has to be replaced by a constant. The peak area I_s is given by Eq. (2)

$$I_s = N \int_0^{\infty} [1 - e^{-(D/v\tau)(1-\alpha v\tau)}] e^{-\lambda t} dt = N\tau \quad (2)$$

and the sum of both peaks areas is: Eq. (3)

$$I_0 + I_s = N \left\{ \int_0^{\infty} [1 - \alpha v\tau e^{-(D/v\tau)(1-\alpha v\tau)}] e^{-\lambda t} dt + Ce^{D\alpha} \right\} \quad (3)$$

The experimental ratios of the unshifted area to the total area were fitted with the following formula:

$$I_0 / (I_0 + I_s) = \frac{e^{-(D/v\tau)(1-\alpha v\tau)} + Ce^{D\alpha}}{\int_0^{\infty} [1 - \alpha v\tau e^{-(D/v\tau)(1-\alpha v\tau)}] e^{-\lambda t} dt + Ce^{D\alpha}} \quad (4)$$

$d_0 = d - D$, τ and C being the free parameters. The solid curve in the right half of Fig. 1 corresponding to $\tau = 314 \pm 22$ psec represents the best fit for the 160-keV level in ^{47}Ti . This lifetime value is in agreement with the values $\tau = 320 \pm 100$ ps and $\tau = 294 \pm 24$ ps obtained by direct timing^{8,9)}.

Only the unshifted peak for $146 \rightarrow 88$ keV γ -transition in ^{47}V was analysed, due to the presence of another strong line in the γ -spectrum near the shifted peak. For each plunger setting, the area of the unshifted peak was normalised by the constant N which was deduced from the ^{47}Ti data and Eq. (3). The normalised areas were fitted with the following formula:

$$I_0 = K \int_0^{\infty} [e^{-(D/v\tau_1)(1-\alpha v\tau_1)} + C_1 e^{D\alpha}] e^{-\lambda t} dt \quad (5)$$

where K is a normalisation constant independent of D . The value found for K by fitting the ^{47}Ti data was taken as a constant and only three free parameters were left: K , τ_1 and C_1 . The decay curve for the 88 keV γ -transition is shown in Fig. 2. The fit to the data yields a value of $\tau_1 = 630 \pm 130$ psec.

The X-ray peaks from a Pb impurity were observed in the γ -spectra. The $K(\beta_1)$ -line is clearly seen in the left side of Fig. 3 which displays the γ -ray data for the 88-keV transition in ^{47}V for three plunger distances D . The peak in the middle of the spectra is composed of both the unshifted 88-keV γ -ray and the $K(\beta_2)$ -line from Pb. Therefore only the shifted component I_s was analysed. The feeding of the 88-keV level was almost completely due to the 56-keV γ -transition. Only a few percent of the feeding arose from the 259-keV level whose mean-life is 90 psec. Ignoring this small contribution, the normalised intensities I_s were fitted by the following formula:

$$I_s = K' \left\{ \tau_1 \left[1 - e^{-(D/v\tau_1)}(1 - \alpha v \tau_1) \right] + \tau_2 \left[1 - e^{-(D/v\tau_2)}(1 - \alpha v \tau_2) \right] \right\} \quad (10)$$

where the index 1 and 2 refer to the 119-keV level and 88-keV level respectively. A first fit with K' , τ_1 and τ_2 as free parameters, yielded values of $\tau_1 = 0.45$ psec and $\tau_2 = 1.20$ nsec. A second fit with only K' and τ_2 as free parameters yielded a value of $\tau_1 = 1.23 \pm 0.16$ nsec.

The errors on the lifetimes include possible errors due to de-orientation effects. These additional errors, whose maximum values ranged from 2% to 5%, were evaluated using Eq. (23) from Ref. 10. The parameters λ_K and A_K of this equation were determined in the same way as Brown et al. (11).

3. CONCLUSIONS

Mean-lives of $\tau = 1.23 \pm 0.16$ ns and $\tau = 0.63 \pm 0.13$ ns for the 88-keV $5/2^-$ and 146-keV $7/2^-$ states in ^{47}V are obtained in the present work. It should be noted that the lifetime value for the 88-keV state is in slight disagreement with an earlier upper limit of 1 ns obtained by the pulsed-beam technique in the $^{47}\text{Ti}(p, n\gamma)$ reaction (3).

Table I summarizes the reduced transition probabilities deduced from the present work. The dipole character of the $5^{-} 2^{-} \rightarrow 4^{-} 2^{-}$ transition is known from a conversion coefficient measurement¹². The $7^{-} 2^{-} \rightarrow 6^{-} 2^{-}$ E2 transition strength is obtained by using the experimental branching ratio² of 0.016 ± 0.005 for the 146-keV level to ground state decay. The $7^{-} 2^{-} \rightarrow 6^{-} 2^{-}$ M1 transition rate is calculated assuming that the corresponding B(E2) ≤ 100 W.u.

It has been shown in a previous work²⁾ that whereas the $1f_{7/2}^{-}$ picture (calculation A) fails to reproduce the excitation energies of the low lying negative parity states, a dramatical change occurs when $1f_{7/2}^{-}(2p_{1/2}^{-} 2p_{3/2}^{-} 1f_{5/2}^{-})$ configurations (calculation B) are also allowed. The same trend is observed for the calculated transition probabilities reported in table I. It will be discussed in a forthcoming paper devoted to a detailed shell model study covering $1f_{7/2}^{-}$ conjugate pairs, including ^{47}V and $^{46}\text{Cr}^{-1}$.

The authors would like to express their appreciation to R. Freeman for stimulating comments.

Table 1 summarizes the reduced transition probabilities deduced from the present work. The dipole character of the $5^{-} 2^{-} \rightarrow 2^{-}$ transition is known from a conversion coefficient measurement¹². The $7^{-} 2^{-} \rightarrow 2^{-}$ E2 transition strength is obtained by using the experimental branching ratio¹² of 0.016 ± 0.005 for the 146-keV level to ground state decay. The $7^{-} 2^{-} \rightarrow 2^{-}$ M1 transition rate is calculated assuming that the corresponding B(E2) ≤ 100 W.u.

It has been shown in a previous work²⁾ that whereas the $1f_{7/2}$ picture (calculation A) fails to reproduce the excitation energies of the low lying negative parity states, a dramatical change occurs when $1f_{7/2}^b(2p_{1/2}^b 2p_{3/2}^b 1f_{5/2}^b)$ configurations (calculation B) are also allowed. The same trend is observed for the calculated transition probabilities reported in table 1. It will be discussed in a forthcoming paper devoted to a detailed shell model study covering $1f_{7/2}$ conjugate pairs, including $4^{+}V$ and $4^{+}Cr^{12}$.

The authors would like to express their appreciation to R. Freeman for stimulating comments.

REFERENCES

1. W. Kutschera, R. B. Huber, C. Signorini and P. Blasi, Nucl. Phys. A210, 531 (1973).
2. N. Schulz and M. Toulemond, Nucl. Phys. A230, 401 (1974).
3. P. Blasi, T. Fazzini, A. Giannattempo, R. B. Huber and C. Signorini: Nuovo Cim. 15A, 521 (1973).
4. L. Mulligan, S. L. Tabor, L. K. Fifield and R. W. Zurmühle, Bull. Amer. Phys. Soc. 20, 732 (1975).
5. W. Kutschera, W. Dehnhardt, O. C. Kistner, P. Kump, B. Povh and H. J. Sann, Phys. Rev. C5, 1658 (1972).
6. D. R. Goosman and R. W. Kavanagh, Phys. Letters 24E, 507 (1967).
7. L. K. Fifield, J. W. Noé, D. P. Balamuth and R. W. Zurmühle, Nucl. Phys. A204, 516 (1973).
8. R. E. Holland and F. J. Lynch, Phys. Rev. 121, 1464 (1961).
9. D. C. S. White, W. J. McDonald, G. C. Neilson and D. A. Hutcheon, Nucl. Instr. Meth. 121, 439 (1974).
10. K. W. Jones, A. Z. Schwarzschild, E. K. Warburton and D. B. Fossan, Phys. Rev. 179, 1773 (1969).
11. B. A. Brown, D. B. Fossan, J. M. McDonald and K. A. Snover, Phys. Rev. C9, 1033 (1974).
12. W. Menti, Helv. Phys. Acta 40, 981 (1967).
13. E. Pasquini et al., in preparation.

Table I.

Experimental and theoretical transition probabilities in ^{47}V .

J_i	J_f	Transition character	Reduced transition probabilities		
			Exp.	Calc. A	Calc. B
5/2	\rightarrow 3/2	M1 (μ_N^2)	0.07 ± 0.01	0.01	0.07
7/2	\rightarrow 5/2	M1 (μ_N^2)	0.45 ± 0.09	0.02	0.07
7/2	\rightarrow 3/2	E2 ($e^2 \text{fm}^4$)	315 ± 118	41	78

FIGURE CAPTIONS

1. Recoil-distance data for the 160-keV \rightarrow g. s. γ -transition in ^{47}Ti . The left portion of the figure displays γ -spectra taken at three different plunger distances $D(\text{mm})$. The right portion of the figure is a semi-logarithmic plot of $I_0 (I_0 + I_s)$ versus D . The solid curve represents the best fit of Eq. (4) to the data.
2. Decay curve for the 146-keV \rightarrow 88-keV γ -transition in ^{47}V . The solid curve represents the best fit of Eq. (5) to the data.
3. Recoil-distance data for the 88-keV \rightarrow g. s. γ -transition in ^{47}V . The left portion of the figure displays γ -spectra taken at three different plunger distances $D(\text{mm})$. The X-ray lines are due to a Pb contaminant. The right portion of the figure is a semi-logarithmic plot of I_s versus D . The solid curve represents the best fit of Eq. (6) to the data.

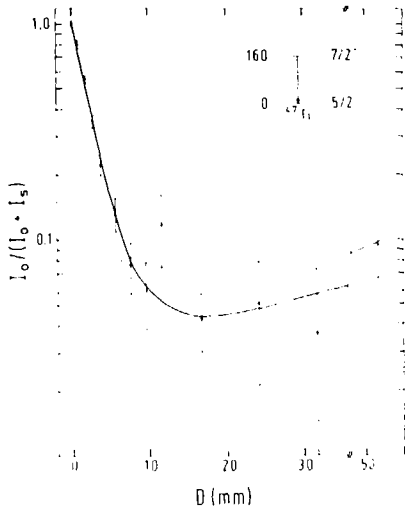
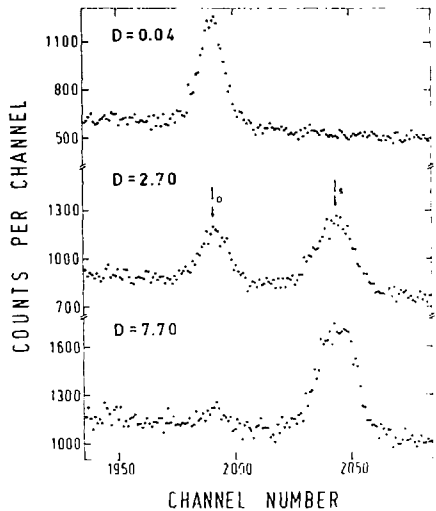


Fig 1

I_0 (ARBITRARY UNITS)

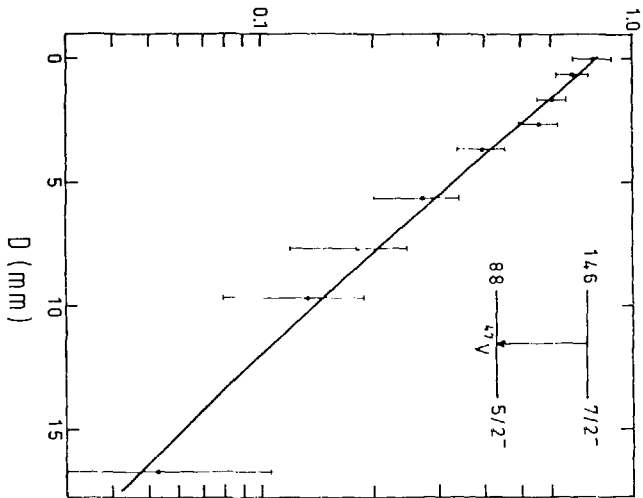


Fig. 2

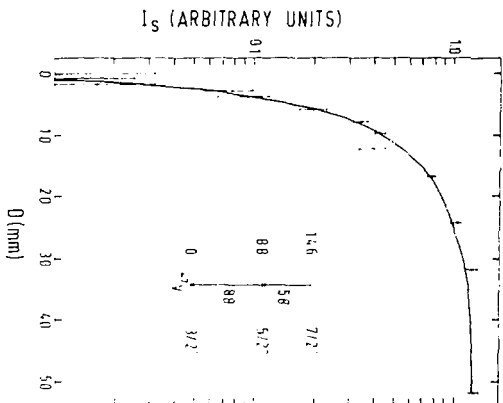
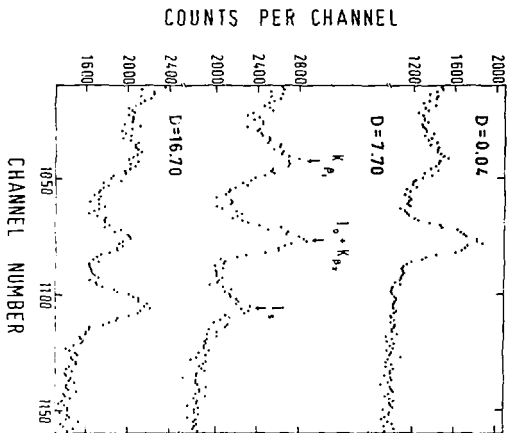


Fig. 3